JGR Atmospheres

RESEARCH ARTICLE
10.1029/2023JD038804

Changing Nature of High-Impact Snowfall Events in Eastern North America

Christopher D. McCray[1], Gavin A. Schmidt[2], Dominique Paquin[1], Martin Leduc[1], Zhaoyue Bi[3], Mohammad Radiyat[3], Carolyn Silverman[3], Matthew Spitz[3], and Brian R. Brettschneider[4]

[1]Ouranos Consortium, Montréal, QC, Canada, [2]NASA Goddard Institute for Space Studies, New York, NY, USA, [3]Data Science Institute, Columbia University, New York, NY, USA, [4]National Weather Service - Alaska Region, Anchorage, AL, USA

Key Points:

- Mean annual snowfall is projected to decrease across most of eastern North America as the Earth continues to warm
- The most intense high-impact snowfall events currently observed will continue to occur in a warmer climate
- A larger percentage of yearly snowfall is likely to fall during a few large events near the Canada-United States border

Supporting Information:

Supporting Information may be found in the online version of this article.

Correspondence to:

C. D. McCray,
mccray.christopher@ouranos.ca

Citation:

McCray, C. D., Schmidt, G. A., Paquin, D., Leduc, M., Bi, Z., Radiyat, M., et al. (2023). Changing nature of high-impact snowfall events in Eastern North America. *Journal of Geophysical Research: Atmospheres*, *128*, e2023JD038804. https://doi.org/10.1029/2023JD038804

Received 3 MAR 2023
Accepted 10 JUN 2023

Abstract Snowstorms cause substantial disruption in the eastern United States and Canada each winter. While reductions in annual snowfall are projected over most of this region due to anthropogenic global warming, daily snowfall extremes that have the greatest impact may not decrease in the same manner. We examine changes to two extreme snowfall metrics: the 95th percentile of daily snowfall (SF95, cm) and the number of events during which 10% of the mean annual snowfall is exceeded during a single day (TC10, events yr^{-1}). We explore changes to these metrics in two ensembles of the fifth-generation Canadian Regional Climate Model, including four 0.22° (≈25 km) simulations driven by different coupled general circulation models as well as the higher-resolution (0.11°, ≈12 km) ClimEx ensemble, driven by 50 members of a large initial-condition ensemble of one global model. We find that while mean annual snowfall is projected to decrease over our domain, SF95 is projected to remain relatively constant, suggesting that the most extreme daily snowfalls currently observed are likely to occur even in a warmer future climate. The region of the largest TC10 values exhibits a northward shift, with a larger percentage of annual snowfall occurring during a few large events along the U.S.-Canada border. These projected changes to the nature of snowfall events may have important socioeconomic consequences in this densely populated region of North America.

Plain Language Summary Snowstorms affect the highly populated regions of the northeastern United States and southeastern Canada every winter, disrupting ground and air travel and resulting in substantial socioeconomic impacts. Understanding how climate change may impact snowstorms is necessary for this region to prepare for the future. We explore how snowstorms in these regions may change in a future, warmer world using two sets of climate model simulations. We find that yearly total snowfall is likely to decrease over most of this region, with the largest declines to the south and smaller declines farther north. Despite these decreases, we find that the snowfall amounts that currently occur during the largest snowstorms are still likely to occur even in a much warmer future climate. Finally, we examine snowstorms that produce a large percentage of the annual snowfall during a single event. We find that the region where these big snowstorms relative to the yearly snowfall occur most often will shift northward in the future. In summary, while yearly snowfall is likely to decrease nearly everywhere in eastern North America, significant snowstorms will continue to occur, and some regions will see more of their yearly snowfall during a few large events.

1. Introduction

Snowstorms can have severe socioeconomic effects on the highly populated regions of the eastern United States and Canada (e.g., Kocin & Uccellini, 2004). Heavy snowfall can make surface and air transportation difficult or impossible as a result of slippery surfaces. Wet snow can weigh down and break trees and power lines, and shoveling this heavy snow can lead to health risks. Heavy snow loads can also result in roof and building collapse. Changnon and Changnon (2006) estimated that from 1949 to 2000, snowstorms caused $21.6 billion (year 2000 U.S. dollars) in insured property losses in the U.S. with the greatest losses occurring in the Northeast ($7.3 billion) and Southeast ($4.1 billion) regions. Several severe snowstorms have impacted this region in recent years. For example, a January 2016 blizzard prompted Washington, D.C. and New York City to implement driving bans and shut down public transportation (Glenza, 2016). In December 2022, a historic lake-effect snow event produced more than 50 in. (≈130 cm) of snow over a 4-day period in Buffalo, New York, stranding motorists and resulting in fatalities (Kilgannon et al., 2022).

The definition of a "snowstorm" may vary between regions—while substantial disruption may require large snowfall amounts over northernmost regions such as southeastern Canada, areas that are less accustomed to heavy snowfalls may be paralyzed by only a few centimeters of snow. One example is the January 2014 snow event, during which ≈2 in. (≈5 cm) of snow resulted in thousands of flight cancellations and traffic crashes that stranded motorists for up to 20 hr in Atlanta and surrounding regions (Burns, 2014; Samenow, 2014; Severson, 2014).

Future snowfall changes may be driven by several, sometimes competing, factors. First, with continued anthropogenic greenhouse gas emissions, additional warming may decrease snowfall and increase the percentage of precipitation falling as rain. On the other hand, in regions where temperatures remain sufficiently cold for snow, increased precipitation due to higher atmospheric water vapor content and greater precipitation intensity may result in increased snowfall. Additionally, changes to atmospheric circulation patterns (e.g., Barnes & Screen, 2015; Cohen et al., 2018, 2019; Francis & Vavrus, 2012; Marciano et al., 2015) as well as related teleconnections such as the North Atlantic Oscillation (NAO)/Northern Annular Mode (NAM) (e.g., Gillett & Fyfe, 2013; Hurrell, 1995; McKenna & Maycock, 2021; Thompson & Wallace, 1998) may alter storm tracks, cyclone frequency and intensity and the associated snowfall climatology. In the Great Lakes region, where lake-effect snow events produce a large percentage of annual snowfall (e.g., Eichenlaub, 1970), snowfall changes are also complicated by trends in lake temperatures and ice coverage (e.g., Notaro et al., 2015).

Several studies have found that over much of the Northern Hemisphere, warming surface temperatures are the primary effect leading to decreasing annual snowfall amounts (Kapnick & Delworth, 2013). For example, over Eastern North America, Krasting et al. (2013) found projected decreasing mean annual snowfall trend over the 21st century everywhere except northern Québec, using 18 Coupled Model Intercomparison Project Phase 5 (CMIP5) general circulation models (GCMs). Despite strong agreement on decreasing mean annual snowfall among recent studies, potential changes to heavy snowfall events over eastern North America remain highly uncertain (IPCC, 2021). Using 20 CMIP5 simulations, O'Gorman (2014) found that while future mean snowfall is likely to decrease with warming over the Northern Hemisphere, the magnitude of extreme snowfall (defined as the 99.99th percentile of daily snowfall) changes are very small. O'Gorman (2014) noted that heavy snowfall tends to occur within a narrow temperature range (around −2°C), and that this range remains constant in future climates. As a result, the magnitude of the most extreme snowfall events is unlikely to change, though the frequency of occurrence of these events may change as the probability of surface air temperatures in the optimal temperature range for extreme snowfall is modified as the Earth warms.

Following O'Gorman (2014), several studies have examined heavy snowfall changes using a diversity of methods. Studies using GCMs have generally identified projected decreased in annual snowfall over most of eastern North America, with either near-zero projected change or slight increases in the most extreme events defined using either percentiles (e.g., 99.9th) or thresholds (20 cm, 30 cm) (Danco et al., 2016; Janoski et al., 2018; H. Chen et al., 2020). Similarly, Zarzycki (2018) applied a storm tracking algorithm to 35 CESM large ensemble members to identify snowstorms and found large decreases in the frequency of minor snowfall events, but smaller changes to moderate and extreme snowstorms. The more severe snowstorms may even temporarily increase in frequency during the middle of the century as extreme precipitation becomes more frequent and temperatures remain sufficiently cold for snow.

While GCMs are physically consistent with the imposed forcings, they typically are run using a coarse horizontal grid–0.75°–3.75° for the atmospheric component of the CMIP5 simulations used by Danco et al. (2016), ≈0.5°–2.5° for the CMIP6 simulations presented in IPCC (2021). This coarse resolution and associated physical parameterizations result in reduced skill at reproducing the precipitation climatology (e.g., IPCC, 2021). This is particularly true over regions of complex terrain, as regional topography is poorly represented. To overcome the challenges posed by coarse GCMs, statistical downscaling, bias correction and pseudo-global warming (PGW) techniques have also been used to examine extreme snowfall changes. Notaro et al. (2014) statistically downscaled nine CMIP3 GCMs, finding decreases in annual snowfall but stagnation or increases in the largest daily snowfall events and mean snowfall intensity over eastern North America. More recently, Quante et al. (2021) examined changes in daily snowfall in an ensemble of bias-corrected and statistically downscaled CMIP6 simulations following the high-emissions SSP5-8.5 scenario. Over eastern North America, they found a steady decrease in mean daily snowfall through the 21st century, except for certain regions of Québec. However, the value of the 99.9th percentile of daily snowfall is projected to remain nearly constant and even increase over most of Québec and Labrador.

The PGW approach has allowed for an examination of the thermodynamic response of snowfall events to global warming at very high resolution. This technique typically involves driving a regional climate model with a reanalysis data set for which certain variables have been perturbed using a climate change signal calculated from one or multiple GCMs (e.g., Brogli et al., 2023; Liu et al., 2017). Comparison with a control simulation driven by the unperturbed reanalysis data allows for an examination of the climate change signal in the RCM. Ashley et al. (2020) applied this technique using two Weather Research and Forecasting (WRF) model simulations, tracking "swaths" of grid points with positive SWE. They found a significant decline in all snowstorm metrics examined (total area, duration and magnitude). While the most extreme 90th percentile SWE portions of the snowstorms also declined over most regions, some regions of the northeastern U.S. and much of southern Canada showed either no change or increasing frequency of these events during January and February. G. Chen et al. (2021) also used the PGW approach, but instead explored possible changes to 93 observed snowstorms using 5 km WRF simulations. Under the warmer perturbed climate, snowfall along the coast decreased for nearly all events and increased further inland for some events. G. Chen et al. (2021) found a substantial decrease in moderate and heavy snowfall compared with the observed climate as snow was converted to rain.

Only one study has presented results from traditional dynamical downscaling experiments using regional climate models (RCMs) driven by GCMs for changes in heavy snowfall events over eastern North America. Notaro et al. (2015) used an RCM to downscale two CMIP5 GCMs following RCP8.5 to a 25-km grid mesh. However, their focus was on possible changes to lake-effect snow, and results were therefore presented for grid points surrounding the Great Lakes Basin. Over this region, they found mean decreases in annual snowfall and daily snowfall frequency in both simulations by the end of the 21st century. The frequency of heavy lake-effect snow events is also projected to decrease except near Lake Superior during the mid-21st century, as increased precipitation associated with warming counteracts the increased potential for lake-effect snow resulting from increased precipitation and reduced lake ice coverage.

Brogli et al. (2023) demonstrated that the PGW approach produces a very similar pattern of precipitation change to a traditional RCM simulation (using the same GCM to calculate the PGW deltas as that used to force the RCM), although measures related to cyclone activity like eddy kinetic energy (EKE) exhibit different patterns of change. While their PGW experiment showed little 500-hPa EKE change over the European domain, the traditional dynamical downscaling experiment projected reduced EKE associated with a reduced meridional temperature gradient under polar amplification. Here, we aim to compliment existing GCM- and PGW-based studies on extreme snowfall using traditional dynamical downscaling techniques that incorporate both thermodynamic and large-scale dynamical responses to warming. First, we identify changes in a set of four simulations of the fifth-generation Canadian Regional Climate Model (CRCM5) over North America at 0.22° grid spacing driven by four different GCMs. We additionally examine changes in the high-resolution (0.11°) 50-member ClimEx ensemble (Leduc et al., 2019) of CRCM5 driven by members of the CanESM2 large ensemble (Fyfe et al., 2017). The use of these two ensembles allows us to identify regions of robust change in the frequency and intensity of extreme snowfall events.

2. Data and Methods

2.1. Regional Climate Model Simulations

We explore snowfall using two sets of simulations produced using the CRCM5 (Martynov et al., 2013; Separovic et al., 2013). The first is an ensemble of four simulations from the North American component of the Coordinated Regional Climate Downscaling Experiment (NA-CORDEX, Mearns et al., 2017) at 0.22° (≈25 km) horizontal grid spacing, with lateral boundary conditions provided by four CMIP5 GCMs: CanESM2 (Arora et al., 2011), MPI-ESM-LR (Giorgetta et al., 2013), GFDL-ESM2M (Dunne et al., 2012), and CNRM-CM5 (Voldoire et al., 2013). This data set allows us to identify the robustness of projected changes to the driving GCM chosen. These simulations are described in McCray, Paquin, et al. (2022).

Additionally, we employ the 50-member ensemble from the ClimEx project, which investigates the effects of climate change on extreme meteorological and hydrological events and their implications for water management in Bavaria, Germany and Québec, Canada (Leduc et al., 2019). The ensemble consists of 50 transient simulations of the CRCM5 at 0.11° (≈12 km) grid spacing, driven by different members of the CanESM2 large ensemble (CanESM2-LE) from 1950 to 2100 (Fyfe et al., 2017). We use this ensemble of model simulations to estimate

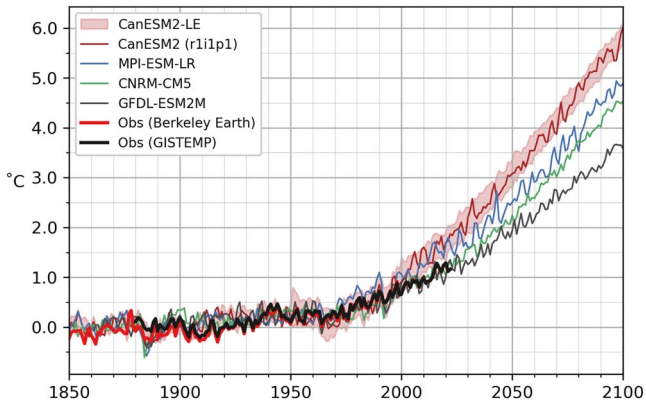

Figure 1. Global mean surface temperature anomaly (relative to 1850–1900) for the four general circulation models discussed in the text (thin solid lines) and the spread of CanESM2 large ensemble members (red shading). Two observational datasets are also plotted through 2022 for reference: Berkeley Earth (Rohde & Hausfather, 2020) (thick red line) and GISTEMP (Lenssen et al., 2019) (thick black line). Observational anomalies are first calculated with respect to the 1986–2005 mean, and the IPCC (2021) best estimate of warming from 1850–1900 to 1986–2005 (0.69°C) is then added to each data set to ensure an equivalent reference period.

both the forced signal of change and the envelope of natural (or internal) variability. This ensemble is unique in both the number of ensemble members for a regional model and the existence of the full transient simulation (1950–2100). This allows for an unprecedented look at sharp regional detail at the statistics of relatively rare snow events. For both the CRCM5-CORDEX and ClimEx ensembles used here, external forcing is driven by observed concentrations of greenhouse gasses and aerosols from 1950 to 2005, and RCP8.5 (van Vuuren et al., 2011) subsequently to 2100.

For each of the two ensembles, we examine evaluation simulations driven by ERA-Interim reanalysis (Dee et al., 2011) data. These simulations are on the same horizontal grids as their corresponding historical and future climate simulations. The CRCM5–ClimEx evaluation simulation runs from 1979 to 2013 and the CRCM5–CORDEX evaluation simulation from 1979 to 2017. We use these simulations to evaluate the ability of the two CRCM5 configurations to reproduce the observed 1980–2009 climate.

Equilibrium climate sensitivity among the driving GCMs ranges from 2.4 K (GFDL-ESM2M) to 3.7 K (CanESM2) (Andrews et al., 2012). The climate state by the end of the 21st century therefore varies substantially among the simulations, with the global mean surface temperature ≈2° warmer in the CanESM2 than the GFDL-ESM2M by 2100 (Figure 1). Rather than averaging values among such differing climate states, we examine results in the context of global warming levels (GWLs) following the technique of Nikulin et al. (2018). As in McCray, Paquin, et al. (2022), we calculate GWL periods as the 30-year period during which the centered moving average of the global mean surface temperature anomaly relative to the 1850–1900 mean in the driving GCM attains the given temperature threshold for the first time. Periods for each GWL and driving GCM are provided in Table S2. The CNRM-CM5 and GFDL-ESM2M do not reach +4°C for any 30-year period before the end of the simulations in 2100, so only MPI-ESM-LR and CanESM2-driven simulations (including ClimEx) are presented for this level. An additional benefit of this method is that our results are largely independent of scenario selection (e.g., Hausfather et al., 2022), with consistent changes for a given GWL between RCP4.5 and 8.5.

Separovic et al. (2013) evaluated the intrinsic behavior of the CRCM5 using a simulation driven by ERA-Interim reanalysis (Dee et al., 2011) and comparing the results with observations. Over our study region, they found the CRCM5 to have a wintertime cold bias (1–4°C) over the southeastern U.S. and a near-zero bias over much of northeastern North America except for far northern Québec and Labrador, where cold biases of the magnitude of those over the Southeast were found. Wintertime precipitation biases were also relatively small, with a slight wet bias over portions of the eastern U.S. and western Québec.

Both CRCM5 configurations examined here include a coupled lake model (FLake, Mironov et al., 2010) which supports a realistic representation of lake-effect precipitation, though the one-dimensional nature of FLake ignores three-dimensional processes that may impact lake ice coverage and lake surface temperature which strongly impact lake-effect snow processes (e.g., Baijnath-Rodino & Duguay, 2019; Martynov et al., 2012). An evaluation of the CRCM5 using FLake shows a general warm bias for Great Lakes temperatures, leading to an early spring warming, a too slow autumn cooling and shorter periods of ice-coverage (Martynov et al., 2012). Given these biases and the complexity of lake-effect snow, we focus here primarily on locations affected by synoptic-scale snowstorms.

2.2. Snowfall Observations

We examine snowfall observations (recorded in mm snowfall) from the Global Historical Climatology Network (GHCN)-Daily (Menne et al., 2012). We select stations with fewer than 10% of missing days per year for at least 24 of the 30 years (80%) of our 1980–2009 reference period. Calculations of station statistics are performed using only years with <10% of missing days for a given station.

We define a snowfall event as daily snowfall (24-hr snowfall starting at 00 UTC) exceeding 1.0 cm. We tested several thresholds (0.1 cm, 1.0 cm, 2.0 cm). The only metric shown here (Section 2.4) that is meaningfully

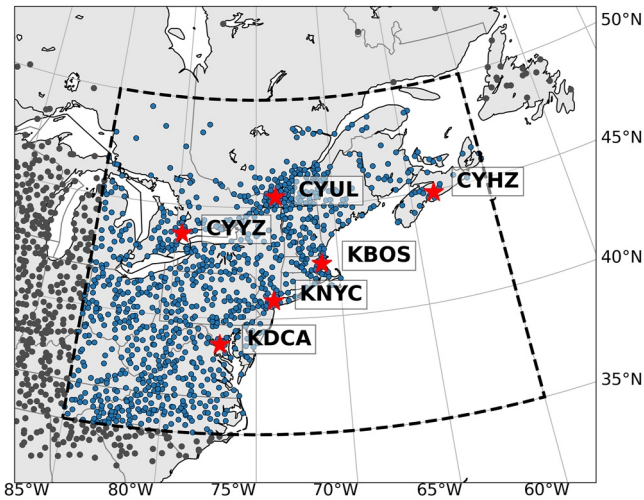

Figure 2. Map of the study domain and observing stations used for model evaluation. Stations within the inner domain are identified by blue circles, while stations in the extended outer domain used for interpolation are identified by gray circles. Stations discussed in the text are denoted by the red stars.

impacted by the threshold is the 95th percentile of daily snowfall, which increases as the threshold increases, but the spatial pattern remains the same. We have also examined 2-day snowfall events rather than single day events, and while magnitudes of the statistics change, the spatial patterns are largely independent of the number of days chosen. We therefore concentrate on daily snowfall events for simplicity. We restrict our analysis to stations with at least 10 snowfall events (daily snowfall >1.0 cm) to avoid calculations of our snowfall metrics using a very small sample.

A total of 1025 stations meet these criteria within a domain spanning 85°W–60°W longitude and 35°N–50°N latitude (Figure 2) which includes the highly populated Mid-Atlantic and Northeast regions of the U.S. and the Québec City-Windsor corridor within which more than half of Canada's population resides. Though statistical analysis is restricted to these stations, an additional 988 stations in a broader outer domain (95°W–50°W longitude and 30°N to 60°N latitude) are used for interpolation and plotting of observed values for visual comparison with model output. We interpolate observations to a 0.2° latitude-longitude grid using the MetPy (May et al., 2022) "interpolate_to_points" function with the radial basis function (RBF) method. For most of the domain, the representation of our variables varies little when using different interpolation techniques due to high station density. The primary exception is over regions north of ≈47°N where few stations are available (Figure 2), so interpolated observations are likely to be less representative of reality over this region.

In addition, we present changes at six individual stations within the domain: Toronto, Ontario (CYYZ); Montréal, Québec (CYUL); Halifax, Nova Scotia (CYHZ); Boston, Massachusetts (KBOS); New York City, New York (KNYC); and Washington, D.C. (KDCA) (Figure 2). We select the nearest grid point to each station in model output for further analysis.

2.3. Model Snowfall

Precipitation in CRCM5 is partitioned into phase (rain, snow, freezing rain or ice pellets) according to the Bourgouin (2000) precipitation-type algorithm applied online at each model time step (every 5 min for CRCM5-ClimEx, 10 min for CRCM5-CORDEX simulations). This algorithm calculates the positive (>0°C) and negative (<0°C) areas of the vertical dry-bulb temperature profile, with area proportional to the pressure depth and mean temperature of a given layer. Snow is diagnosed if the positive area associated with above-freezing air at the surface is less than 5.6 J kg^{-1}, resulting in limited melting of hydrometeors. Limitations of this technique include its exclusive use of the vertical dry-bulb temperature profile, with no consideration for humidity. However, Reeves et al. (2014) noted this algorithm to be skillful at detecting snow, while McCray, Thériault, et al. (2022) found the Bourgouin (2000) method was able to closely reproduce the observed freezing rain climatology with CRCM5.

Comparison of modeled and observed snowfall is complicated because CRCM5 snowfall is output not as snow depth, but as the precipitation flux attributed to snow, and is therefore in units of kg m^{-2} s^{-1} which can be converted to mm SWE (1 kg m^{-2} s^{-1} = 1 mm d^{-1} SWE). Snow density is quite variable (depending on temperature and other meteorological conditions) and no single value can accurately translate from the mass flux diagnostics in the model output to the snowfall depth that is the diagnostic of most interest (Baxter et al., 2005; Roebber et al., 2003). Historically, a snow density of 100 kg m^{-3} was assumed (a snow-to-liquid ratio (SLR) of 10:1), but observations suggest a range of densities from as low as 10 kg m^{-3} to 300 kg m^{-3} (with higher densities associated with warmer temperatures). Baxter et al. (2005) found mean SLRs in the U.S. ranging from 7:1 in the Southeast to 15:1 in the Northern Plains and in the regions east of the Great Lakes where lake-effect snow is most common. Additionally, snow measurement practices have changed over time in the National Weather Service Co-operative network (Kunkel et al., 2009; Lawrimore et al., 2014). While a more sophisticated method to calculate SLRs could be applied, this would add a level of uncertainty beyond the scope of this manuscript. We therefore convert daily SWE output from our simulations to snowfall using a simple 10:1 ratio (1 mm SWE = 1 cm snowfall).

2.4. Selected Snowfall Metrics

We aim to define spatially varying grid point statistics that capture extreme snowfall characteristics based on magnitude and rarity. Our first metric is mean annual snowfall. We first sum daily snowfall from 1 January to 31 December of each year, and then calculate the mean for 30-year periods, 1980–2009 for the recent past climate and the 30-year period during which the +2°, +3°, and +4°C GWLs are attained.

We also identify two metrics that highlight snowfalls that have the greatest impact. The first is SF95, the 95th percentile of daily snowfall among events (i.e., among only days with >1 cm of snowfall) calculated over a 30-year period. SF95 provides perspective on the magnitude of the largest snowfalls observed at a given location. We focus on SF95 rather than larger thresholds that are more extreme but produce rarer events and therefore noisier statistics.

Our final metric is Threshold Count 10% (TC10), the mean annual frequency of events exceeding 10% of the 30-year climatological mean annual snowfall at a given location. These events may involve small snowfall amounts in an absolute sense but may be impactful given their relatively large magnitude with respect to the mean annual snowfall at a particular location. The 10% threshold is calculated independently for each 30-year period, such that the threshold for a TC10 event changes in the future climate. We have tested several percentage thresholds. Larger thresholds (e.g., 25%) yield too few snow events and noisy statistics, while smaller thresholds lead to statistics that approach those of the mean annual snowfall climatology and thus add little value.

The two metrics (SF95 and TC10) differ in that the first focuses on events that are large with respect to other events, while the second is focused on events that are large with respect to the mean annual snowfall at a given location. Regions with few, but large snowfall events will be highlighted by TC10, even where SF95 is small. Conversely, changes in the magnitude of large snowfalls that are independent of the number of events are better captured by SF95.

3. Historical Snowfall Statistics

We first evaluate the ability of the CRCM5 to reproduce the observed snowfall climatology. We compare GHCN-Daily observations with the evaluation simulation of each ensemble driven by ERA-Interim using CRCM5 at 0.22° and 0.11° grid spacing.

3.1. Mean Annual Snowfall

The spatial pattern of mean annual snowfall in both the CRCM5-CORDEX (Figure 3b) and CRCM5-ClimEx (Figure 3c) strongly resembles the observed pattern (Figure 3a). The largest annual mean values (>500 cm yr^{-1}) occur over northeastern Québec, Newfoundland and Labrador, as well as in regions east of Lakes Ontario and Erie. Despite the limitations related to FLake discussed in Section 2.1, the region of lake-effect snow is reproduced by both simulations, with the local maximum slightly better-defined in the CRCM5-ClimEx simulation (Figure 3c).

The Pearson correlation coefficient between mean annual snowfall in observations and each evaluation simulation is strong, with $r = 0.91$ and 0.92 for CRCM-CORDEX and CRCM5-ClimEx, respectively (Figures 4a and 4d). Both simulations have a positive mean bias, with a slightly higher bias for CRCM5-CORDEX (36.6 cm yr^{-1}) than CRCM5-ClimEx (32.2 cm yr^{-1}), with slightly better root-mean-square error (RMSE) values for CRCM5-ClimEx as well. The largest errors are primarily found at high-elevation stations (e.g., Mount Washington, New Hampshire) or stations in the lake-effect snowbelts east of the Great Lakes in New York and Ontario. At these stations, the CRCM5 tends to underestimate snowfall. For the 29 stations with elevations above 750 m, mean bias is −21.5 cm yr^{-1} (−34.4 cm yr^{-1}) for the CRCM5-ClimEx (CRCM5-CORDEX) simulation, while for the 996 stations above this elevation the simulations overestimate mean annual snowfall (mean biases of +33.8 and +38.6 cm yr^{-1}, respectively).

3.2. SF95

Unlike mean annual snowfall, the amount of snow associated with extreme snowfall events (SF95) is largest near the Atlantic coastline from Virginia northeastward to Nova Scotia, with the largest values exceeding 24 cm in some locations (Figure 3d). This pattern is associated with a common wintertime storm track along the Atlantic

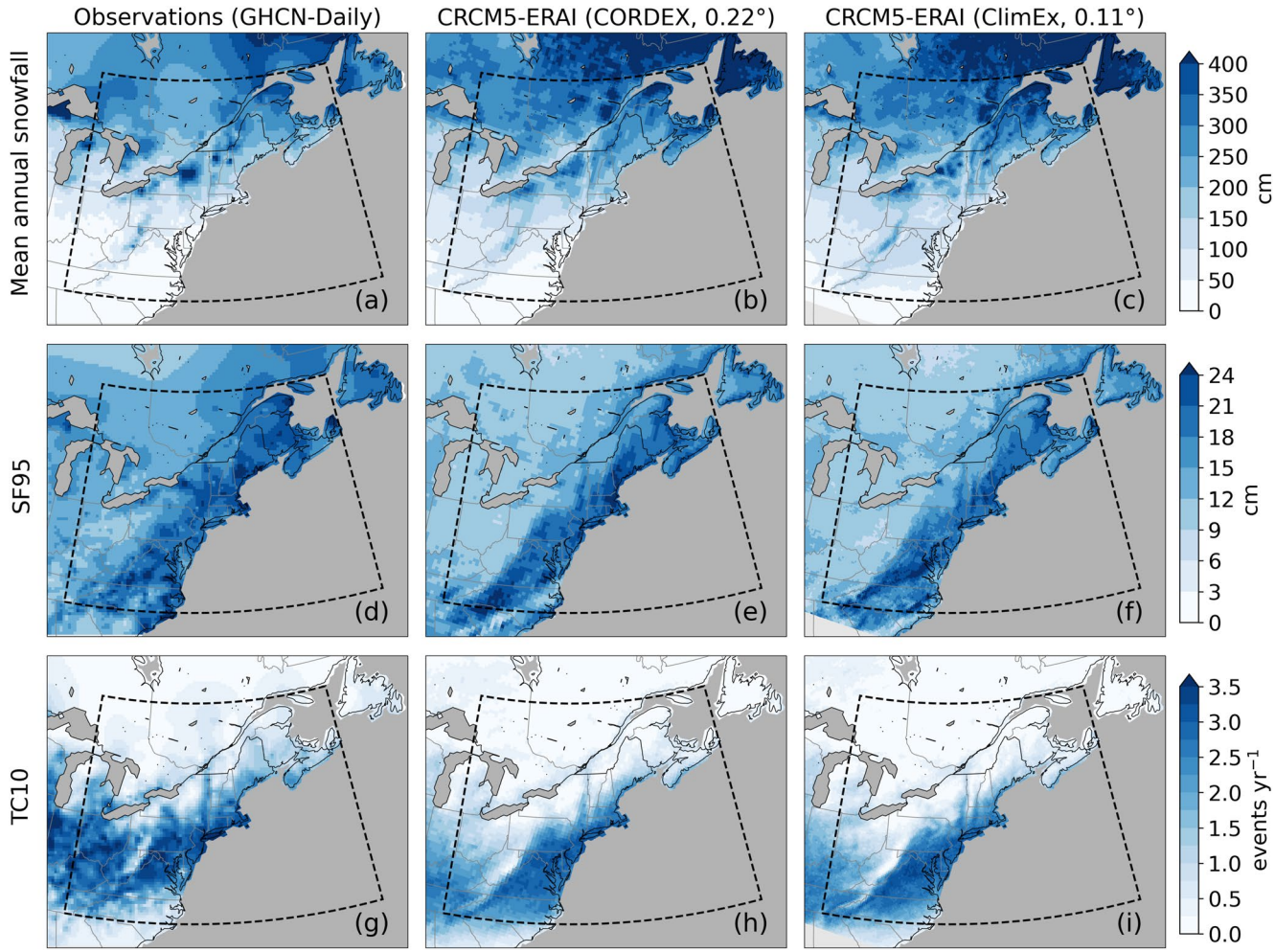

Figure 3. Statistics of the three snowfall metrics for 1980–2009 in observations (a, d, and g), CRCM5–ERA-Interim at 0.22° (b, e, and h) and CRCM5–ERA-Interim at 0.11° (c, f, and i). Statistics presented include mean annual snowfall (cm, a–c), the 95th percentile of daily snowfall (cm, d–f) and the mean number of events exceeding 10% of the mean annual snowfall (events yr^{-1}, g–i).

coast, with cyclone generation often associated with baroclinicity enhanced by the intersection of cold, Arctic air masses with the Gulf Stream (e.g., Kocin & Uccellini, 2004). Both evaluation simulations reproduce this spatial pattern (Figures 3e and 3f), though observed values west of the Appalachians are underestimated by both simulations. This may be due to the higher SLR values typical of this region, ≈12–15:1 according to Baxter et al. (2005), which would result in higher amounts for a given liquid equivalent than the 10:1 ratio used here.

The point comparisons indicate strong spatial correlation between observed and simulated SF95 values, with $r = 0.70$ for CRCM5-CORDEX and $r = 0.73$ for CRCM5-ClimEx (Figures 4b and 4e). However, there is greater spread in the values compared with mean annual snowfall (Figures 4a and 4d). The 95th percentile of daily snowfall is noisier than the mean, and can vary depending on the period chosen in the climatology due to internal variability. SF95 is also quite dependent on the minimum event threshold. For example, for the CRCM5-CORDEX simulation, the domain-averaged mean of SF95 is 14.7 cm with our 1.0 cm minimum threshold, compared with 10.8 cm for a 0.1 cm event threshold. Both simulations have a negative bias for SF95, in contrast to the positive mean annual snowfall bias. Potential explanations for this bias include an insufficient representation of the mesoscale physical processes associated with extreme snow, as well as our 10:1 snowfall ratio assumption.

3.3. TC10

The pattern of TC10 (Figure 3g) is distinct from either mean annual snowfall or SF95. TC10 events are rare, with the greatest frequencies only slightly exceeding 3 events yr^{-1}. These maximum values are found in the southernmost

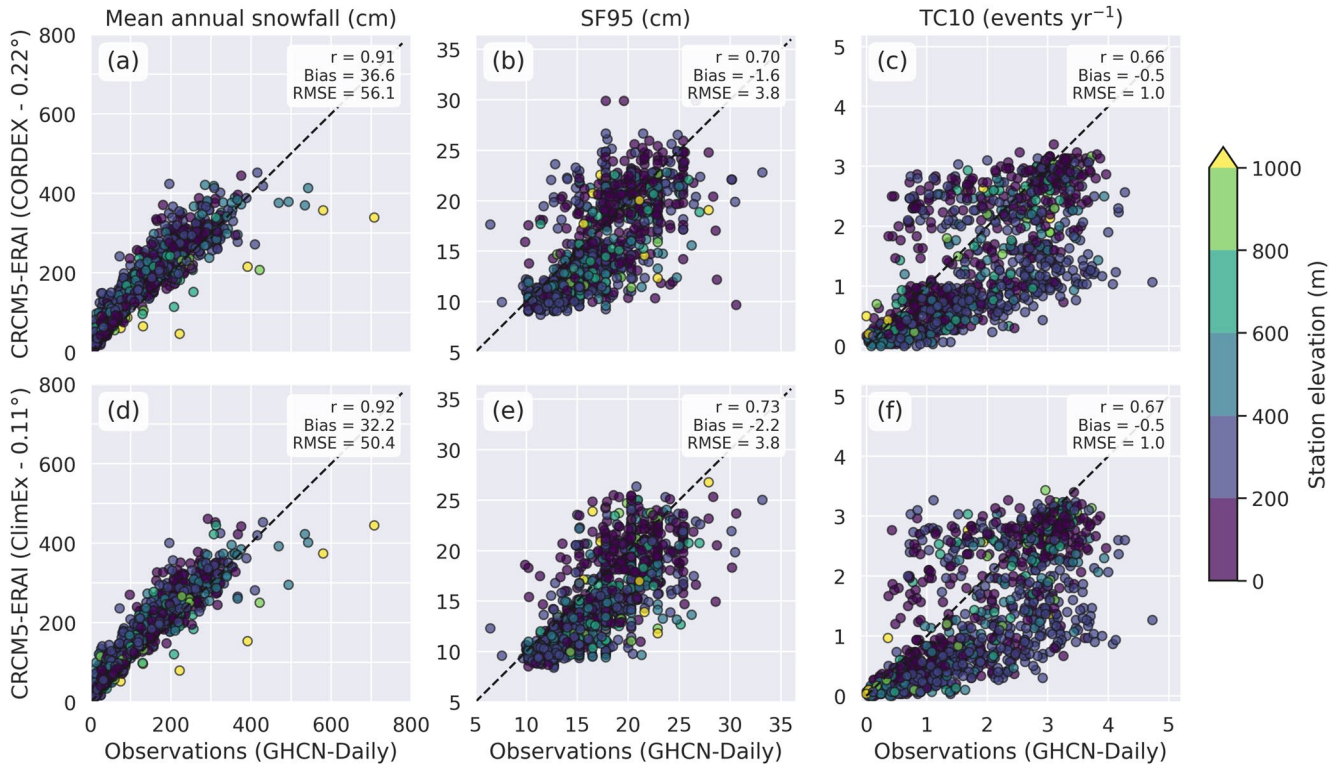

Figure 4. Comparisons of observed and simulated values at the nearest model grid point to each of the 1025 stations in our inner domain in the CRCM5–ERA-Interim simulations from the 0.22° CORDEX (a–c) and the 0.11° ClimEx (d–f) grids for mean annual snowfall (cm) (a and d), the 95th percentile of daily snowfall (cm) (b and e), and the number of events exceeding 10% of the mean annual snowfall (events yr^{-1}) (c and f). Also indicated are the Pearson correlation coefficient *r*, mean bias (cm) and root mean square error (RMSE, cm) for each simulation and metric.

areas of the domain that observe less annual snowfall than northern regions. Notably, areas in the highly urbanized Northeast Corridor (Virginia northeastward to Massachusetts) have large numbers of events annually.

Both reanalysis-driven CRCM5 simulations reproduce the general spatial pattern of TC10 east of the Appalachians, though the region of maximum values is shifted slightly southward compared with observations (Figures 3g–3i), and maximum values are slightly smaller. The correlation coefficients between observed and simulated values are lower than for the other two metrics–$r = 0.66$ and 0.67 for CRCM-CORDEX and CRCM5-ClimEx, respectively.

Point comparisons between observed and simulated TC10 values suggest several clusters of values (Figures 4c and 4f), and we find these clusters to be regional in nature. Simulated and observed TC10 values are strongly correlated for the 345 stations east of −75°W ($r = 0.91$ and 0.92 for CRCM-CORDEX and CRCM5-ClimEx, respectively). Correlations are much weaker for the 680 stations west of −75°W ($r = 0.53$ and 0.54, respectively). This is associated with the strongly underestimated TC10 values in both simulations west of the Appalachians, over portions of western Pennsylvania, West Virginia, Ohio, and eastern Kentucky (Figures 3g–3i).

3.4. Individual Cities

Examination of values at our six stations of interest highlights the varying nature of snowfall among different regions of our domain (Table 1). The northernmost cities of Halifax and Montréal have the greatest mean annual snowfall (217 and 204 cm, respectively), but the magnitude of the most extreme events (SF95) is largest at Boston (22.1 cm) and New York City (21.6 cm) which have substantially lower mean annual snowfall amounts than Montréal or Halifax. The lowest SF95 value is at Toronto (12.5 cm), far removed from the East Coast storm track, followed by Montréal (17.2 cm). The region with the highest frequency of TC10 events is further south over the Mid-Atlantic, with the largest values at New York City (3.4 events yr^{-1}) and Washington, D.C. (3.2 events yr^{-1}). The lowest frequency of these events occurs at Halifax and Montréal (1.0 and 1.1 events yr^{-1}, respectively), where the mean annual snowfall is greatest.

Table 1
Observed Values (1980–2009) for Mean Annual Snowfall (cm), the 95th Percentile of Daily Snowfall (SF95, cm) and the Number of Events Exceeding 10% of the Mean Annual Snowfall (TC10, Events yr^{-1}) at Six Stations in Our Domain

	Mean annual snowfall (cm)	SF95 (cm)	TC10 (events yr^{-1})
Toronto, Ontario (CYYZ)	110	12.5	1.6
Montréal, Québec (CYUL)	204	17.2	1.1
Halifax, Nova Scotia (CYHZ)	217	18.7	1.0
Boston, Massachusetts (KBOS)	110	22.1	2.9
New York City, New York (KNYC)	62	21.6	3.4
Washington, D.C. (KDCA)	38	18.4	3.2

4. Projected Changes

Given the overall ability of the CRCM5 at both 0.11° and 0.22° to reproduce the observed climatology of our snowfall metrics, we now explore the projected changes to these metrics in a future climate. Each driving GCM has biases that are inherited by the RCM, resulting in slightly different snowfall patterns among our simulations. For mean annual snowfall, the CRCM5–GFDL-ESM2M simulation has the largest positive bias, while simulations driven by CanESM2 have slightly negative biases. Observed and simulated mean annual snowfall remains well-correlated, with r ranging from 0.86 to 0.91. Additional information on the differences among individual simulations can be found in Section S1 in Supporting Information S1.

4.1. Mean Annual Snowfall

Consistent with prior studies (Danco et al., 2016; Janoski et al., 2018; Kapnick & Delworth, 2013; Krasting et al., 2013; Notaro et al., 2014), mean annual snowfall is projected to decrease in the future over most of the domain for both the CRCM5-CORDEX and CRCM5-ClimEx ensembles. All four CRCM5-CORDEX simulations agree on decreasing annual snowfall at +2°C of warming over most of our domain, with the largest relative decreases (30%–40%) in southernmost regions and along the coast from North Carolina to Massachusetts (Figure 5a). Further north over southern Québec, models agree on more modest relative declines (10%–20%), however because this region has large (>200 cm yr^{-1}) mean annual snowfall for the past climate (Figures 3a–3c), small relative changes represent absolute declines of 10–30 cm yr^{-1}. At least 75% of the ClimEx simulations also agree on decreasing annual snowfall over the entire domain at +2°C of warming, with 100% agreement for some grid points (Figure 5d).

Mean annual snowfall is projected to further decline everywhere in the domain at +3°C of global warming, with 100% of CORDEX and ClimEx members agreeing on decreasing snowfall over almost the full domain (Figures 5b and 5e). In the CORDEX simulations, mean declines exceed 50% over coastal regions and much of North Carolina, with declines of 20%–30% extending into southern Québec and Ontario. The ClimEx mean shows decreases exceeding 40% through much of southern New England to Pennsylvania southward.

The two CRCM5-CORDEX simulations with driving GCMs that attain the +4°C GWL by the end of the simulated period (CanESM2 and MPI-ESM-LR) agree on substantial decreases in snow for the entire domain at this GWL (Figure 5c). A similar pattern with stronger declines is found for the CRCM5–ClimEx simulations (Figure 5f). Decreases exceeding 50% are projected over a vast region from North Carolina, through the Mid-Atlantic states, southern New England and the coastal regions of the Canadian Maritimes. The smallest relative changes are found in northern Québec, with declines of <30% in both ensembles.

We illustrate the range of projected changes among our simulations at the major cities indicated in Figure 2. For the 50 CRCM5-ClimEx simulations, we calculate the signal-to-noise ratio S/N at each city for a given indicator x as the ratio of the ensemble mean change for that indicator $\left(\overline{\Delta x}\right)$ to the standard deviation of the change among the 50 ensemble members σ_{ens}, such that

$$\mathrm{S/N} = \frac{\overline{\Delta x}}{\sigma_{ens}} \quad (1)$$

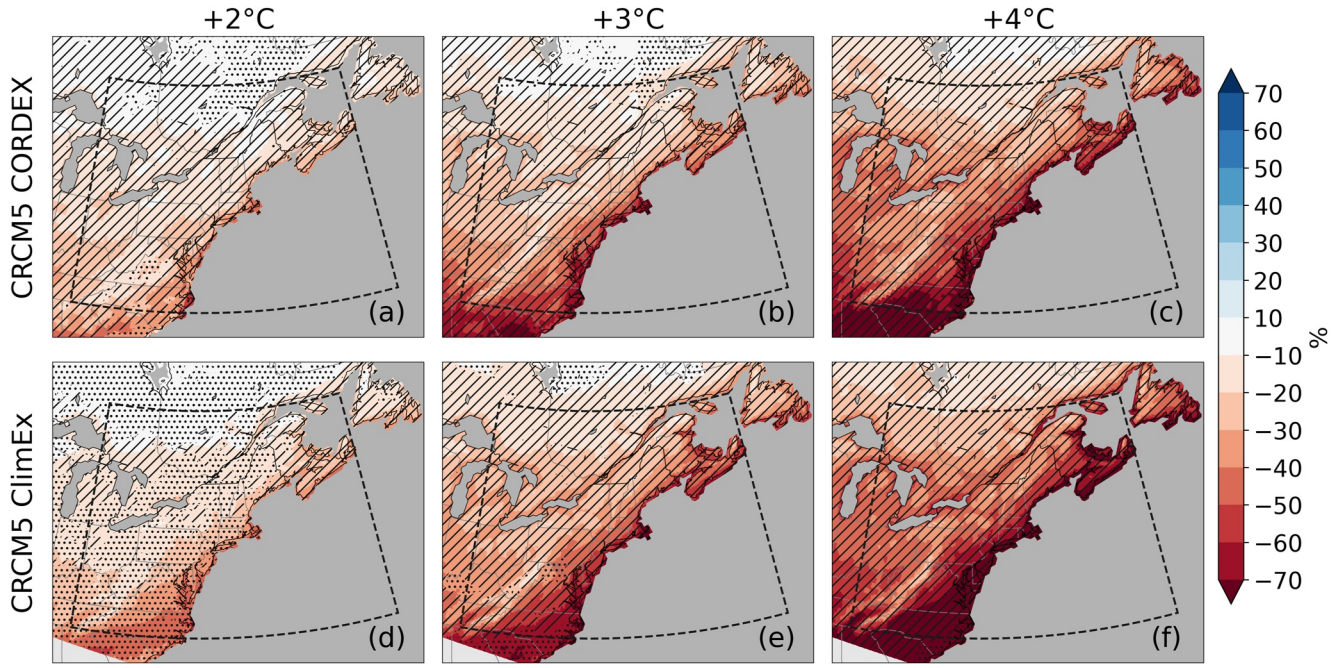

Figure 5. Projected mean relative changes in mean annual snowfall (%) among the (a–c) CRCM5-CORDEX ensemble and (d–f) CRCM5-ClimEx ensemble with respect to the 1980–2009 mean for the +2°C (a and d), +3°C (b and e), and +4°C (c and f) global warming levels. Stippling (hatching) indicates regions where at least 75% (100%) of the four (two for +4°C) CRCM5-CORDEX or 50 CRCM5-ClimEx members agree on the sign of change.

For mean annual snowfall (Figure 6), simulations exhibit strong agreement on projected decreases among all six cities. Relative changes among the individual CRCM5-CORDEX simulations generally fall within the envelope of projections of the 50 CRCM5-ClimEx members. Similar relative changes are projected at Toronto (Figure 6a) and Montréal (Figure 6b), with mean decreases of ≈20% at +2°C, 30% at +3°C, and 50% at +4°C. Projected relative declines are of slightly greater magnitude at Halifax (Figure 6c), ≈30%, 50%, and 70% at +2, +3, and +4°C, respectively. For all six cities, the decreasing signal in CRCM5-ClimEx simulations is strong, with $|S/N| \geq 1.8$ at +2°C and increasing with each additional degree of warming. Halifax exhibits the strongest decreasing signal for all GWLs (Figure 6c), with $S/N = -9.1$ at +4°C.

At Boston, New York City, and Washington, D.C. (Figures 6d–6f), the magnitude of projected declines tends to be greater than at the Canadian cities, though the spread is also larger. For example, at Washington, D.C. and the +2°C GWL, projected changes among the CRCM5-ClimEx simulations range from −62% to +6% (Figures 6f), indicative of substantial internal variability over this region. This variability decreases with additional warming at Boston and New York City (Figures 6d and 6e), though remains large at Washington, D.C. which has the lowest mean annual snowfall in the past climate among the six stations (Table 1). New York City and Washington, D.C. have the weakest signal-to-noise ratios among the six cities, though the signal remains strong ($S/N = -3.6$ at New York City and $S/N = -5.1$ at Washington, D.C. at +4°C).

4.2. SF95

Despite the robust pattern of decreasing annual snowfall, we find few regions where the magnitude of extreme events is projected to change substantially within both ensembles. The spatial pattern of SF95 changes at +2°C contrasts strongly with that for mean annual snowfall, with very few regions of agreement on the sign of change and mean changes near 0 at most grid points for both CRCM5-CORDEX and ClimEx (Figures 7a and 7d).

Even at +3°C of warming, SF95 does not exhibit a coherent pattern of substantial change (Figures 7b and 7e). The only region of agreement on increasing SF95 in both the CRCM5-CORDEX and ClimEx ensembles is over the Québec-Labrador border and Newfoundland, just outside our domain, where mean increases of 1–2 cm are projected. Strong projected decreases in SF95 are found over the Carolinas in the CRCM5-ClimEx mean (Figure 7e), but even these large mean changes are not robust among ensemble members at many grid points.

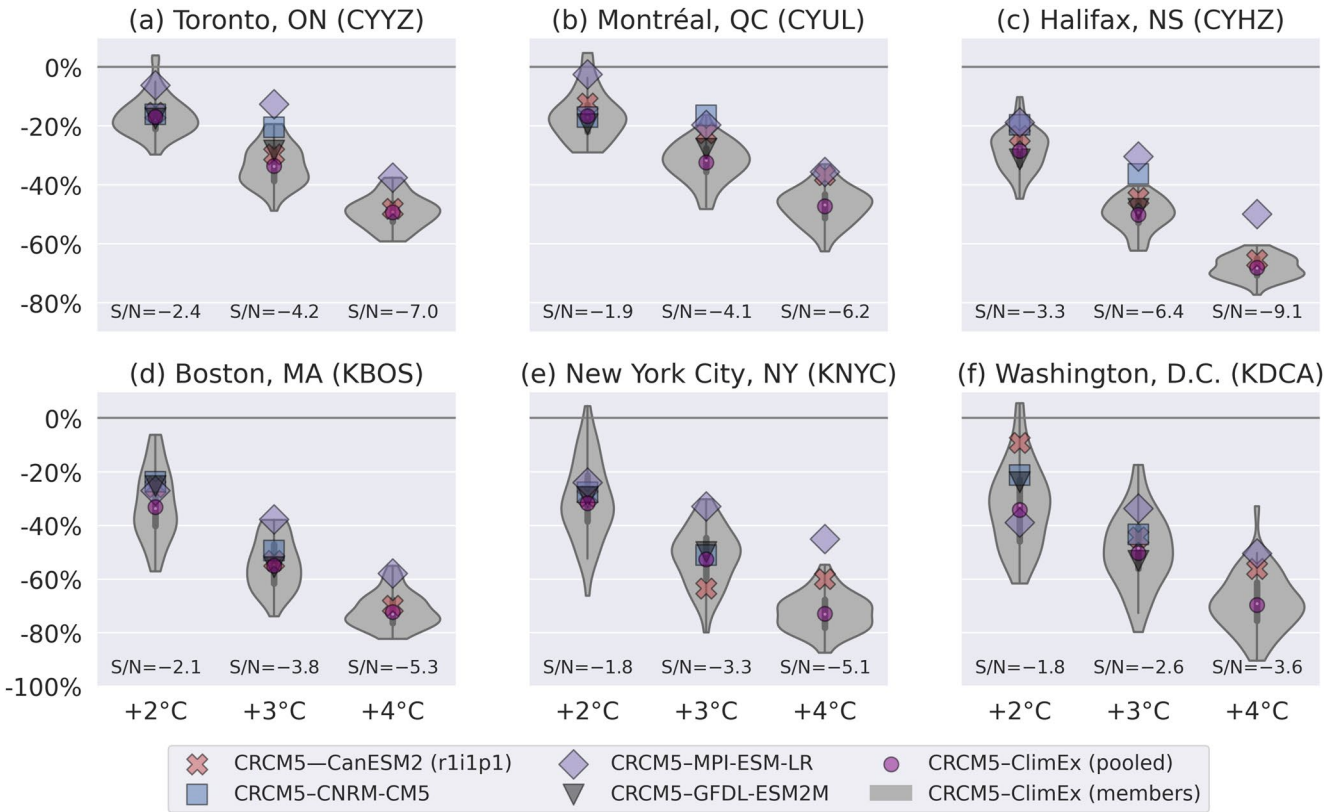

Figure 6. Projected changes to mean annual snowfall (%) at Toronto, Ontario (a); Montréal, Québec (b); Halifax, Nova Scotia (c); Boston, Massachusetts (d); New York City, New York (e); and Washington, D.C. (f) for the three global warming levels. Relative changes with respect to the 1980–2009 mean are plotted for each CRCM5 simulation (symbols indicated in the legend). A kernel density estimation of the distribution of projected changes among the CRCM5-ClimEx simulations is shaded in the gray violin plots generated using the Seaborn package (Waskom, 2021). Within each violin plot, a smaller box plot is included indicating the median (white dot), 25th–75th percentile (dark gray box) and complete range of the CRCM5-ClimEx data (dark gray vertical lines). Values calculated from the pooled data for all 50 ClimEx members are indicated by the purple circles. Signal-to-noise ratio (S/N) calculated from the ClimEx data is indicated under each violin plot.

Otherwise, scattered regions of agreement in the CORDEX simulations appear, though the pattern is quite noisy and not replicated in the ClimEx simulations.

Broader regions of agreement on SF95 changes among the two CORDEX simulations appear at +4°C of global warming, but the spatial pattern remains noisy (Figure 7c). Only two broad regions of at least 75% agreement on the sign of projected SF95 changes appear in the ClimEx simulations (Figure 7f). The first is a region of ≈1–2 cm decreases over much of Ohio and parts of Pennsylvania southward into Kentucky and West Virginia, in the westernmost portion of our domain. The second is the aforementioned region over Newfoundland and surrounding the Québec-Labrador border, where 100% of the ClimEx members now agree on increases (mean of ≈1–3 cm) over some grid points. The 99th percentile of daily snowfall (Figure S2 in Supporting Information S1) shows a very similar pattern to SF95, with few regions of robust change among both ensembles. This more extreme threshold does produce a few additional regions of robust increase over northern New England, New York and Québec, particularly at +4°C.

Robust changes in SF95 are not projected at any of the six cities examined (Figure 8), which partly explains the lack of consistency in change patterns between the CORDEX and ClimEx ensembles. Though some individual members project relatively large changes, distributions at most locations and GWLs peak near 0% among the CRCM5-ClimEx members. The combination of weak signal and large spread results in signal-to-noise ratios less than 1.0 for all cities and GWLs, with the largest values found at Halifax (S/N = 0.8 at +3°C, Figure 8c) and Boston (S/N = −0.7 at +4°C, Figure 8d).

The spread of projected changes even among CRCM5-ClimEx members highlights the difficulty in detecting a signal for SF95. Values can vary greatly among members even for the recent past climate, ranging from 12.2 to

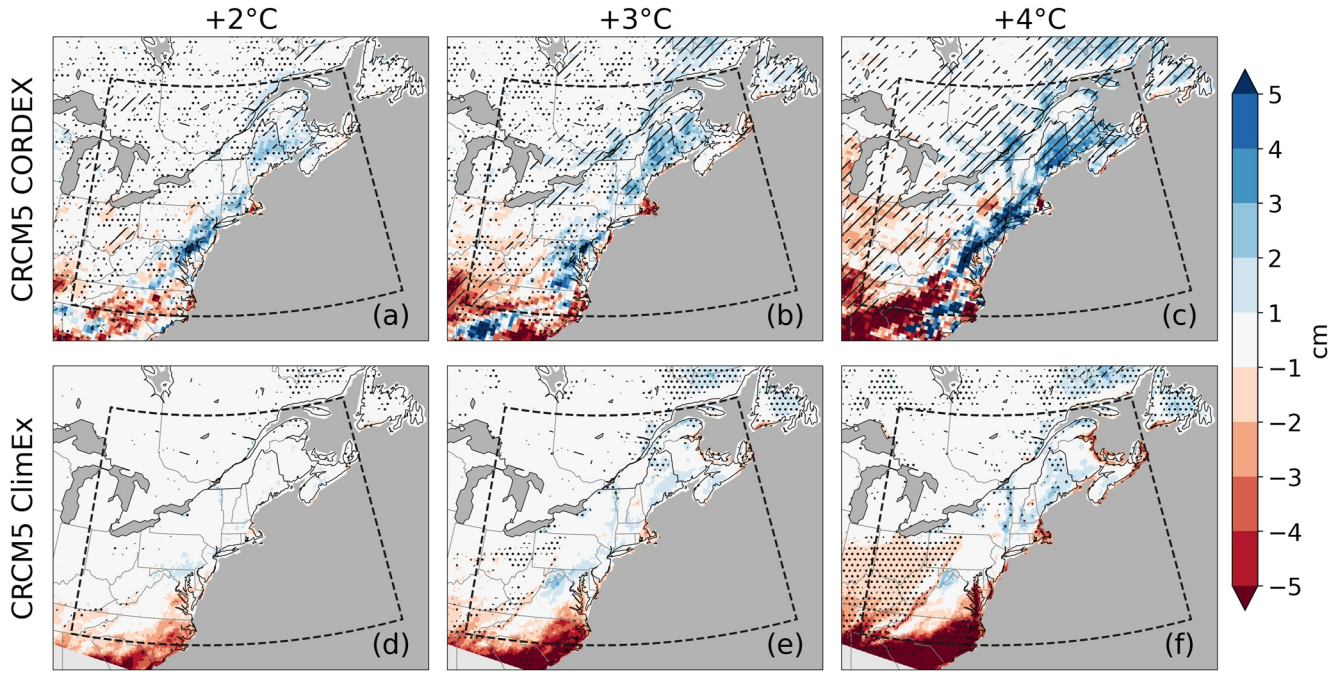

Figure 7. Projected mean changes to the 95th percentile of daily snowfall (cm) relative to 1980–2009 values. Panels and hatching/stippling as in Figure 5.

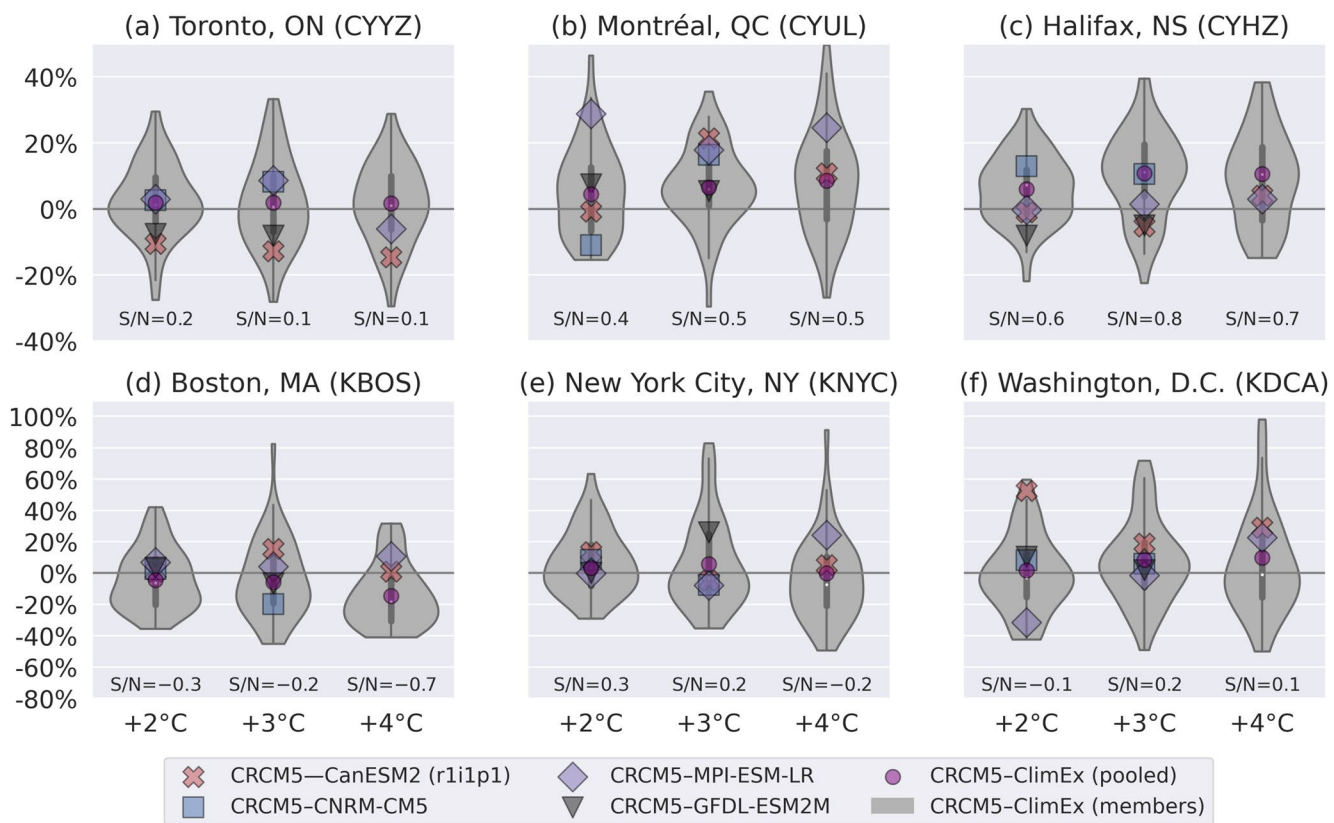

Figure 8. Projected relative changes as in Figure 6 except for the 95th percentile of daily snowfall (%).

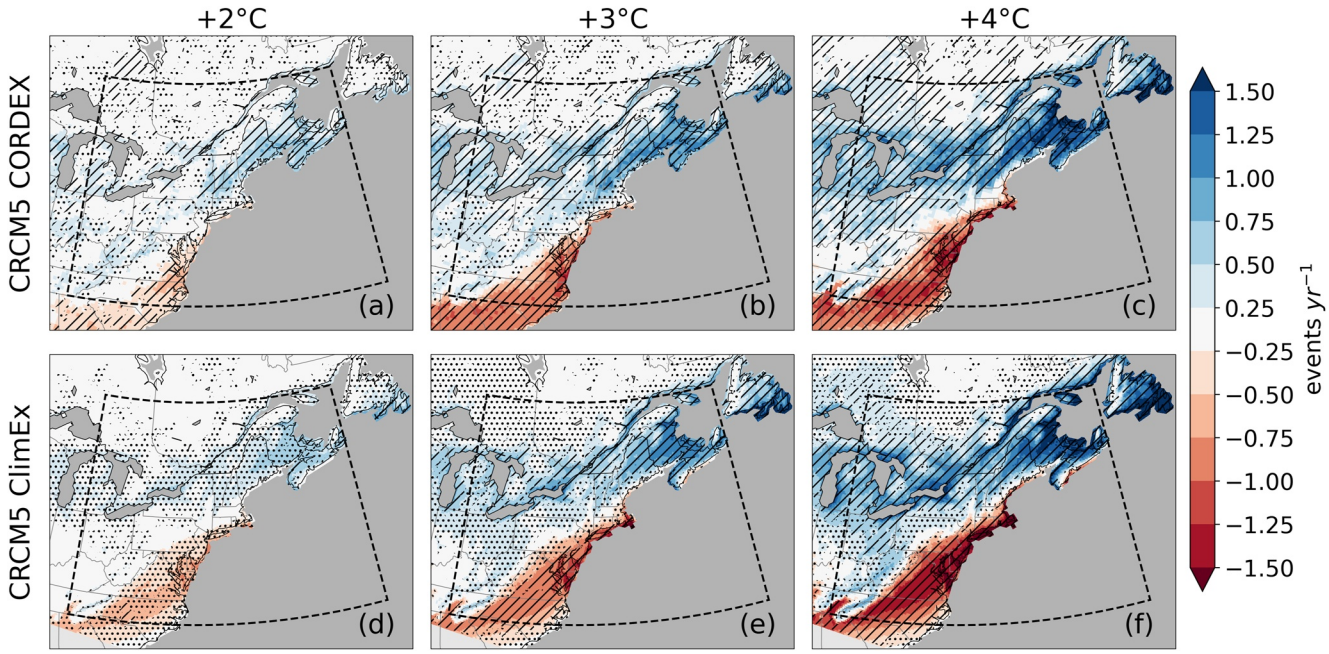

Figure 9. Projected mean changes in the number of annual snowfall events exceeding 10% of the climatological mean annual snowfall (events yr^{-1}). Panels and hatching/stippling as in Figure 5.

16.4 cm at Montréal, for example, Rather than comparing individual members, we can also augment our sample by pooling daily data for all 50 members for the same 30-year period to calculate SF95, providing an effective 1500 years of daily data for the given background climate state. Projected changes derived from the pooled calculation of SF95 are very close to the median of projected changes among the 50 individual members calculated separately (Figure 8). Using the values from this large sample, near-zero change in SF95 is projected for most GWLs and locations. The largest projected change remains Boston, where a 15% decrease in SF95 is projected at +4°C (Figure 8d).

4.3. TC10

The change pattern of the frequency of events exceeding 10% of the annual mean is distinct from those of mean annual snowfall or SF95, with a robust northward shift in the region of largest TC10 values projected at +2°C (Figures 9a and 9d). Though the magnitude of change is initially small, both the CRCM5-CORDEX and CRCM5-ClimEx ensembles agree on an increase in the frequency of TC10 over the Saint Lawrence River Valley in southern Québec and Ontario and over much of central and northern New England. Decreasing TC10 is projected over much of the coastal Mid-Atlantic, from North Carolina northeastward to New Jersey in the ClimEx simulations but restricted to North Carolina and Virginia in the CRCM5-CORDEX ensemble.

The northward shift in TC10 becomes more coherent among the CRCM5-CORDEX members at +3°C, with a band of agreement on increasing values now stretching from Michigan eastward to Nova Scotia (Figure 9b). In the aforementioned regions, 100% of the ClimEx members now agree on the sign of the change at many grid points (Figure 9e). The region of decreasing values also expands northward and increases in magnitude, with decreases stretching from North Carolina to coastal New Jersey in the CRCM5-CORDEX mean (Figure 9b) and reaching into southern New England in the CRCM5-ClimEx mean (Figure 9e).

The region of large TC10 values continues expanding northward at +4°C, with decreases stretching into southern New England in both the CRCM5-CORDEX and ClimEx ensembles (Figures 9c and 9f). The region of coherent increases expands northward through Québec and Ontario in both ensembles. The greatest magnitude of projected increase is found over Atlantic Canada (New Brunswick, Nova Scotia, and Prince Edward Island), where projected mean increases sometimes exceed 1.5 events yr^{-1}. Over these regions, TC10 is currently small, with large mean annual snowfall totals resulting from a mixture of many small snowfalls and a few larger events.

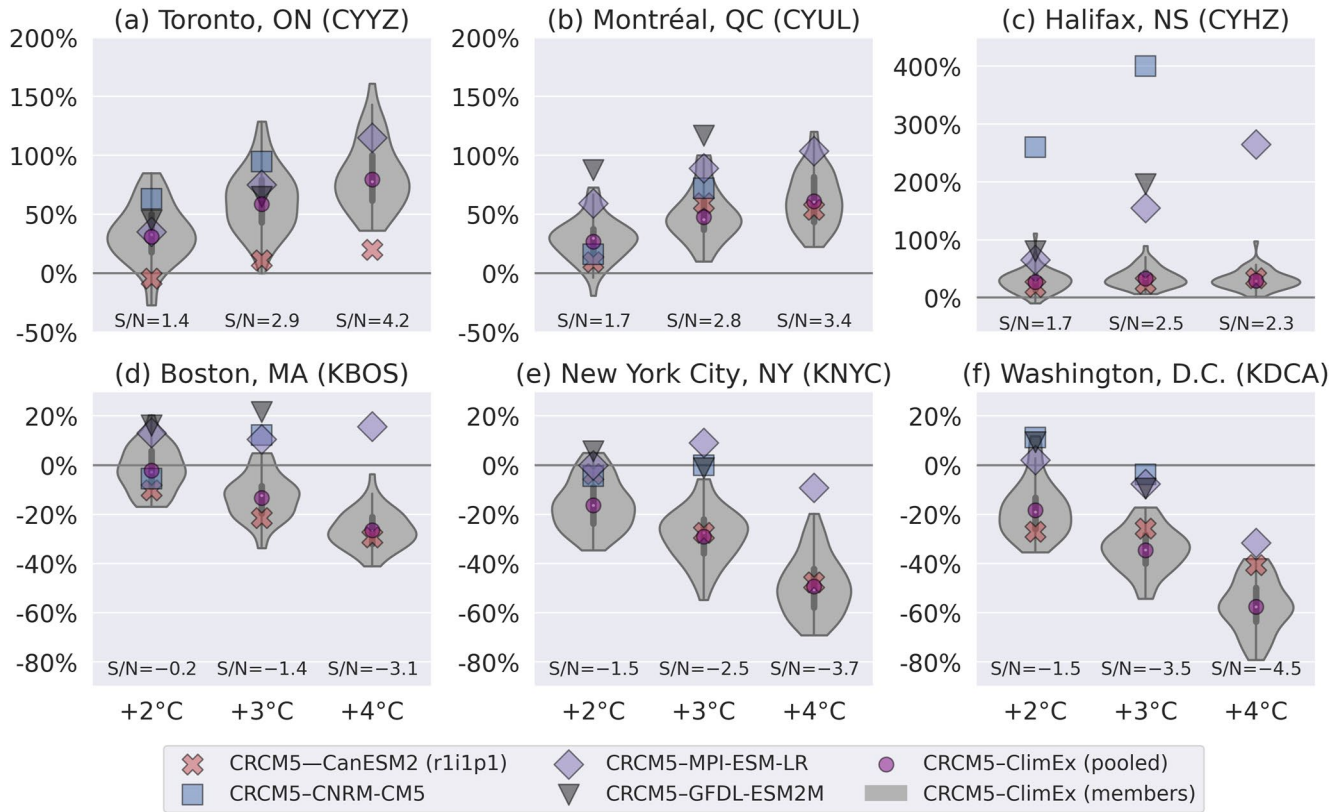

Figure 10. Projected relative changes as in Figure 6 except for the annual number of events exceeding 10% of the mean annual snowfall (TC10).

As TC10 increases, a larger proportion of annual snowfall will fall during a few larger events, as is currently the case over the regions of the Mid-Atlantic.

Among the six cities, the largest projected TC10 increases are found at Halifax (Figure 10c), though magnitudes vary greatly between simulations, largely due to differences in the past climatology of TC10 among the CRCM5–CORDEX simulations (Figures S1k–S1o in Supporting Information S1). The 1980–2009 mean TC10 at Halifax varies from 0.3 events yr^{-1} in CRCM5–CNRM-CM5 and 2.2 events yr^{-1} in CRCM5–CanESM2, resulting in large percentage changes for relatively small absolute increases in CRCM5–CNRM-CM5. More coherent changes are found among the simulations at the other cities. Large increases and strong signals are found at both Toronto (Figure 10a) and Montréal (Figure 10b).

Boston (Figure 10d) is the only city where the magnitude of the signal-to-noise ratio for the CRCM5-ClimEx simulations is less than 1.0 at +2°C, with the sign of projected change varying among simulations. A stronger decreasing signal emerges at +3°C (S/N = −1.4) and +4°C (S/N = −3.1). A robust decreasing signal is also present among the CRCM5-ClimEx simulations at New York City (Figure 10e), though CRCM5-CORDEX simulations disagree on the sign of change until +4°C. Finally, at Washington, D.C. (Figure 10f), simulations are in better agreement on decreasing values of TC10, particularly at +3 and +4°C. Washington, D.C. exhibits the largest mean declines (≈30%–80%) and the strongest decreasing signal (S/N = −4.5) at +4°C of global warming.

5. Concluding Discussion

Prior studies on extreme snowfall changes over eastern North America have primarily relied on output from GCMs (H. Chen et al., 2020; Danco et al., 2016; Janoski et al., 2018; Notaro et al., 2014; O'Gorman, 2014; Quante et al., 2021; Zarzycki, 2018). Some authors applied statistical downscaling and bias correction techniques (Notaro et al., 2014; Quante et al., 2021) to address the challenges posed by the relatively coarse (≥50 km) horizontal grid spacing of these simulations. Except for Zarzycki (2018) and Janoski et al. (2018), these studies also partitioned precipitation into rain and snow based on simple surface air temperature thresholds (e.g., 0°C).

Additional studies (Ashley et al., 2020; G. Chen et al., 2021) employed a pseudo-global warming approach wherein a high-resolution regional model is forced with initial and boundary conditions perturbed with projected thermodynamic changes, though large-scale dynamic changes that may impact the cyclone and snowfall climatologies may not be fully accounted for in this approach (Brogli et al., 2023).

We have filled a gap in the existing literature pertaining to extreme snowfall through the use of two ensembles of high-resolution regional climate simulations. In these simulations, output from coarser GCMs is dynamically downscaled to 0.22° (CRCM–CORDEX) and 0.11° (CRCM5-ClimEx), allowing for an improved representation of local terrain features that can alter precipitation type. Additionally, we identify snow using the full vertical temperature profile via the Bourgouin (2000) precipitation-type algorithm applied at each model time step. Our simulations accurately reproduce the climatology of mean annual snowfall ($r \approx 0.9$) over eastern North America, despite the presence of complex terrain in this region.

In these simulations, we find substantial changes to the nature of snowfall across the eastern United States and southeastern Canada in a future, warmer climate. In agreement with prior studies (e.g., Kapnick & Delworth, 2013; Krasting et al., 2013; Notaro et al., 2014), we find that mean annual snowfall is projected to decrease over nearly all of our domain as temperatures increase and solid precipitation is converted to liquid due to the reduced frequency of subfreezing surface temperatures (Figure 5). Despite marked declines in annual snowfall, we identify few regions of robust change in the magnitude of the 95th percentile of daily snowfall (SF95, Figure 7). The most intense snowstorms currently observed are therefore likely to still occur in a future, warmer climate.

The lack of robust changes to SF95 is consistent with O'Gorman (2014) who suggested the most extreme snowfall amounts are likely to decline much less rapidly than mean snowfall, as heavy snowfall tends to occur at an optimal near-surface temperature which will still occur in a warmer climate. Some regions of agreement are identified among the four CRCM5-CORDEX members, but the absence of agreement among the 50 CRCM5-ClimEx members (Figure 7) and the low signal-to-noise ratios at each station examined (Figure 8) suggest this is likely noise. The *frequency* of snowfall events reaching the magnitude of SF95 (calculated for 1980–2009) is, however, projected to decrease over most of the domain as temperatures in the optimal range occur less frequently with additional warming (Figure S3 in Supporting Information S1).

We have also examined changes to the frequency of extreme events relative to the annual snowfall climatology at a given location through the use of a new metric, TC10, the number of annual snowfall events exceeding 10% of the mean annual snowfall. In locations with little annual snowfall, snowfall amounts associated with TC10 events may be small in an absolute sense, but their impacts may be great depending on the capacity of the location to respond to snowfall. In the recent past climate, observed TC10 is largest over the densely populated regions of the eastern U.S. where large snowfall events occur each winter, but where less snowfall is observed each winter than areas to the north.

We find strong agreement among our simulations on a northward shift in the region of greatest TC10 values with future warming, with a larger percentage of annual snowfall likely to fall during a few, large events near the U.S.-Canada border in the future (Figure 9). As mean annual snowfall decreases, so does the daily snowfall threshold required to count as a TC10 event. Over the major metropolitan areas of the eastern U.S., the number of events that exceed 10% of the mean annual snowfall is projected to decrease despite the decreased threshold (Figure 10). Thus, while intense events should continue to occur (as evidenced by stable SF95 values, Figure 8), heavy snowfall events are projected to become increasingly rare in this region.

The differences in results from our two ensembles, particularly for SF95, highlights the importance of using a large ensemble like ClimEx for analysis of extreme snowfall events, as reliance on individual simulations may result in identification of regions of large projected change that may simply be internal variability. Our use of four driving GCMs and a 50-member initial-condition ensemble of one of those GCMs has allowed us to clearly demonstrate regions where these changes are robust to both driving GCM selection and internal variability, and in the case of SF95, regions where these changes are not robust. Comparison of snowfall changes using a more complete GCM-RCM matrix with multiple RCMs, for example, using the upcoming North American CORDEX simulations driven by CMIP6 GCMs, would allow for a more complete analysis of uncertainty.

One limitation of our study is our use of a fixed 10:1 snow-to-liquid ratio. Given the dependence of snow density on temperature, the regional climatology of these ratios (e.g., Baxter et al., 2005) is likely to evolve in a warmer climate. The impact of these changes is likely to be more important for mean annual snowfall and less important

for the extreme events studied here, given the occurrence of extremes near the −2°C optimal temperature identified by O'Gorman (2014). Still, future studies may consider applying more sophisticated techniques to calculate snow density using model variables (e.g., Roebber et al., 2003). McCrary et al. (2022), for example, examined snow cover and snowpack SWE and their changes in the NA-CORDEX ensemble. In the CRCM5, the Canadian Land Surface Scheme (CLASS, Verseghy, 2000) calculates these variables using a combination of incident snowfall and other processes such as melting and sublimation. Although these additional processes mean these variables are not solely related to snowfall, future studies may consider examining extreme snow depth increases as a proxy for heavy snowfall to account for the impact of snow density on snow amount.

While lake-effect snow is represented in our simulations, we have opted not to examine its changes here and instead focus on cities primarily impacted by synoptic-scale snow events. Future work may consider following (Notaro et al., 2015) and expanding our analysis to regions and cities such as Buffalo, New York that are affected by lake-effect snowfall, which can have substantial socioeconomic consequences (e.g., Kilgannon et al., 2022).

Future work is also warranted examining the dynamic and thermodynamic changes leading to the changing nature of snowfall events identified here. For example, changes in cyclone intensity and frequency (e.g., Colle et al., 2013; Lombardo et al., 2015) and shifts in storm tracks and related teleconnection patterns may partly explain changes to SF95 and TC10. Chartrand and Pausata (2020) found a positive correlation between the monthly NAO index and the frequency of daily snowfall events exceeding the 95th percentile along the U.S. East Coast, with more heavy snowfall events during negative NAO months. In the mean, the CMIP5 and CMIP6 ensembles project an increasing trend in the wintertime NAO index (Gillett & Fyfe, 2013; McKenna & Maycock, 2021), which may suggest fewer SF95 events. However, model uncertainty and internal variability result in different NAO responses to future greenhouse gas emissions among different simulations (McKenna & Maycock, 2021). An application of cyclone tracking techniques such as those used by Zarzycki (2018) could also provide additional clues as to the physical causes of certain changes identified here.

Data Availability Statement

Files containing statistics for each of our three metrics generated for each simulation as well as statistics from the observational data set can be downloaded from McCray et al. (2023) (https://doi.org/10.20383/102.0743). Model output for all CRCM5 simulations used to derive these statistics can be obtained by contacting scenarios@ouranos.ca. CMIP5 simulation output used for calculating global warming levels was downloaded from the Earth System Grid Federation (ESGF) portal hosted by the U.S. Department of Energy Lawrence Livermore National Laboratory (https://esgf-node.llnl.gov/search/cmip5/). Raw daily snowfall observations can be accessed at https://www.ncei.noaa.gov/products/land-based-station/global-historical-climatology-network-daily.

Acknowledgments
Authors C. McCray, D. Paquin, and M. Leduc were supported by Ouranos for this work. They thank their former colleague Sébastien Biner and former Ouranos interns Moussa Bopp and Stéphanie Bergeron for their preliminary work on this topic. G. Schmidt was supported by the NASA Modeling, Analysis and Prediction program. Student input to the project was greatly facilitated by the Data Science Institute at Columbia University and the Masters program in Data Science. The CRCM5 simulations examined here were generated and supplied by Ouranos. CRCM5 computations were made on the Guillimin supercomputer at McGill University, managed by Calcul Québec and Compute Canada. Funding for Guillimin was provided by the Canada Foundation for Innovation (CFI), the ministère de l'Économie et de l'Innovation du Québec (MEI), and the Fonds de recherche du Québec – Nature et technologies (FRQNT). The CRCM5 was developed by the ESCER centre of the Université du Québec à Montréal (UQAM; www.escer.uqam.ca) in collaboration with Environment and Climate Change Canada (ECCC). The production of the ClimEx simulations was funded within the ClimEx project by the Bavarian State Ministry for the Environment and Consumer Protection. We acknowledge ECCC's Canadian Centre for Climate Modelling and Analysis for executing and making available the CanESM2 Large Ensemble simulations used in this study, and the Canadian Sea Ice and Snow Evolution Network for proposing the simulations. Computations with the CRCM5 for the ClimEx project were made on the SuperMUC supercomputer at Leibniz Supercomputing Centre (LRZ) of the Bavarian Academy of Sciences and Humanities. The operation of this supercomputer is funded via the Gauss Centre for Supercomputing (GCS) by the German Federal Ministry of Education and Research and the Bavarian State Ministry of Education, Science and the Arts.

References

Andrews, T., Gregory, J. M., Webb, M. J., & Taylor, K. E. (2012). Forcing, feedbacks and climate sensitivity in CMIP5 coupled atmosphere-ocean climate models. *Geophysical Research Letters*, *39*(9). https://doi.org/10.1029/2012GL051607

Arora, V. K., Scinocca, J. F., Boer, G. J., Christian, J. R., Denman, K. L., Flato, G. M., et al. (2011). Carbon emission limits required to satisfy future representative concentration pathways of greenhouse gases. *Geophysical Research Letters*, *38*(5). https://doi.org/10.1029/2010GL046270

Ashley, W. S., Haberlie, A. M., & Gensini, V. A. (2020). Reduced frequency and size of late-twenty-first-century snowstorms over North America. *Nature Climate Change*, *10*(6), 539–544. https://doi.org/10.1038/S41558-020-0774-4.10.1038/S41558-020-0774-4

Baijnath-Rodino, J. A., & Duguay, C. R. (2019). Assessment of coupled CRCM5–FLake on the reproduction of wintertime lake-induced precipitation in the Great Lakes Basin. *Theoretical and Applied Climatology*, *138*(1–2), 77–96. https://doi.org/10.1007/S00704-019-02799-8

Barnes, E. A., & Screen, J. A. (2015). The impact of Arctic warming on the midlatitude jet-stream: Can it? Has it? Will it? *Wiley Interdisciplinary Reviews: Climate Change*, *6*(3), 277–286. https://doi.org/10.1002/WCC.337

Baxter, M. A., Graves, C. E., & Moore, J. T. (2005). A climatology of snow-to-liquid ratio for the Contiguous United States. *Weather and Forecasting*, *20*(5), 729–744. https://doi.org/10.1175/waf856.1

Bourgouin, P. (2000). A method to determine precipitation types. *Weather and Forecasting*, *15*(5), 583–592. https://doi.org/10.1175/1520-0434(2000)015⟨0583:AMTDPT⟩2.0.CO;2

Brogli, R., Heim, C., Sørland, S. L., & Schär, C. (2023). *The pseudo-global-warming (PGW) approach: Methodology, software package PGW4ERA5 v1.1, validation and sensitivity analyses*. Geoscientific Model Development. https://doi.org/10.5194/gmd-2022-167

Burns, R. (2014). The Day We Lost Atlanta: How 2 lousy inches of snow paralyzed a metro area of 6 million. *Politico Magazine*.

Changnon, S. A., & Changnon, D. (2006). A spatial and temporal analysis of damaging snowstorms in the United States. *Natural Hazards*, *37*(3), 373–389. https://doi.org/10.1007/S11069-005-6581-4

Chartrand, J., & Pausata, F. S. R. (2020). Impacts of the North Atlantic Oscillation on winter precipitations and storm track variability in southeast Canada and the Northeast United States. *Weather and Climate Dynamics*, *1*(2), 731–744. https://doi.org/10.5194/WCD-1-731-2020

Chen, G., Wang, W. C., Cheng, C. T., & Hsu, H. H. (2021). Extreme snow events along the coast of the Northeast United States: Potential changes due to global warming. *Journal of Climate*, *34*(6), 2337–2353. https://doi.org/10.1175/JCLI-D-20-0197.1

Chen, H., Sun, J., & Lin, W. (2020). Anthropogenic influence would increase intense snowfall events over parts of the Northern Hemisphere in the future. *Environmental Research Letters*, *15*(11), 114022. https://doi.org/10.1088/1748-9326/abbc93

Cohen, J., Pfeiffer, K., & Francis, J. A. (2018). Warm Arctic episodes linked with increased frequency of extreme winter weather in the United States. *Nature Communications*, *9*(1), 1–12. https://doi.org/10.1038/s41467-018-02992-9

Cohen, J., Zhang, X., Francis, J., Jung, T., Kwok, R., Overland, J., et al. (2019). Divergent consensuses on Arctic amplification influence on midlatitude severe winter weather. *Nature Climate Change*, *10*(1), 20–29. https://doi.org/10.1038/s41558-019-0662-y

Colle, B. A., Zhang, Z., Lombardo, K. A., Chang, E., Liu, P., & Zhang, M. (2013). Historical evaluation and future prediction of Eastern North American and Western Atlantic extratropical cyclones in the CMIP5 models during the cool season. *Journal of Climate*, *26*(18), 6882–6903. https://doi.org/10.1175/JCLI-D-12-00498.1

Danco, J. F., DeAngelis, A. M., Raney, B. K., & Broccoli, A. J. (2016). Effects of a warming climate on daily snowfall events in the northern Hemisphere. *Journal of Climate*, *29*(17), 6295–6318. https://doi.org/10.1175/jcli-d-15-0687.1

Dee, D. P., Uppala, S. M., Simmons, A. J., Berrisford, P., Poli, P., Kobayashi, S., et al. (2011). The ERA-interim reanalysis: Configuration and performance of the data assimilation system. *Quarterly Journal of the Royal Meteorological Society*, *137*(656), 553–597. https://doi.org/10.1002/qj.828

Dunne, J. P., John, J. G., Adcroft, A. J., Griffies, S. M., Hallberg, R. W., Shevliakova, E., et al. (2012). GFDLs" ESM2 global coupled climate-carbon Earth system models. Part I: Physical formulation and baseline simulation characteristics. *Journal of Climate*, *25*(19), 6646–6665. https://doi.org/10.1175/JCLI-D-11-00560.1

Eichenlaub, V. L. (1970). Lake effect snowfall to the lee of the great Lakes: Its role in Michigan. *Bulletin of the American Meteorological Society*, *51*(5), 403–413. https://doi.org/10.1175/1520-0477(1970)051

Francis, J. A., & Vavrus, S. J. (2012). Evidence linking Arctic amplification to extreme weather in mid-latitudes. *Geophysical Research Letters*, *39*(6). https://doi.org/10.1029/2012GL051000

Fyfe, J. C., Derksen, C., Mudryk, L., Flato, G. M., Santer, B. D., Swart, N. C., et al. (2017). Large near-term projected snowpack loss over the Western United States. *Nature Communications*, *8*(1), 14996. https://doi.org/10.1038/ncomms14996

Gillett, N. P., & Fyfe, J. C. (2013). Annular mode changes in the CMIP5 simulations. *Geophysical Research Letters*, *40*(6), 1189–1193. https://doi.org/10.1002/GRL.50249

Giorgetta, M. A., Jungclaus, J., Reick, C. H., Legutke, S., Bader, J., Böttinger, M., et al. (2013). Climate and carbon cycle changes from 1850 to 2100 in MPI-ESM simulations for the Coupled Model Intercomparison Project phase 5. *Journal of Advances in Modeling Earth Systems*, *5*(3), 572–597. https://doi.org/10.1002/jame.20038

Glenza, J. (2016). *Winter storm brings near-record snow to eastern US as 19 deaths reported – US weather*. The Guardian.

Hausfather, Z., Marvel, K., Schmidt, G. A., Nielsen-Gammon, J. W., & Zelinka, M. (2022). Climate simulations: Recognize the 'hot model' problem. *Nature*, *605*(7908), 26–29. https://doi.org/10.1038/d41586-022-01192-2

Hurrell, J. W. (1995). Decadal trends in the North Atlantic Oscillation: Regional temperatures and precipitation. *Science*, *269*(5224), 676–679. https://doi.org/10.1126/SCIENCE.269.5224.676

IPCC. (2021). *Climate change 2021: The physical science basis. Contribution of Working Group I to the Sixth Assessment Report of the Intergovernmental Panel on Climate Change* [V. Masson-Delmotte, P. Zhai, A. Pirani, S. L. Connors, C. Péan, S. Berger, et al. (Eds.)]. *Cambridge University Press*. https://doi.org/10.1017/9781009157896

Janoski, T. P., Broccoli, A. J., Kapnick, S. B., & Johnson, N. C. (2018). Effects of climate change on wind-driven heavy-snowfall events over Eastern North America. *Journal of Climate*, *31*(22), 9037–9054. https://doi.org/10.1175/jcli-d-17-0756.1

Kapnick, S. B., & Delworth, T. L. (2013). Controls of global snow under a changed climate. *Journal of Climate*, *26*(15), 5537–5562. https://doi.org/10.1175/JCLI-D-12-00528.1

Kilgannon, C., Fadulu, L., Meko, H., & Nir, S. M. (2022). How the Buffalo blizzard became so deadly.

Kocin, P. J., & Uccellini, L. W. (2004). Supplement to a snowfall impact scale derived from Northeast storm snowfall distributions. *Bulletin of the American Meteorological Society*, *85*(2), 194. https://doi.org/10.1175/bams-85-2-kocin

Krasting, J. P., Broccoli, A. J., Dixon, K. W., & Lanzante, J. R. (2013). Future changes in Northern Hemisphere snowfall. *Journal of Climate*, *26*(20), 7813–7828. https://doi.org/10.1175/jcli-d-12-00832.1

Kunkel, K. E., Ensor, L., Palecki, M., Easterling, D., Robinson, D., Hubbard, K. G., & Redmond, K. (2009). A new look at lake-effect snowfall trends in the Laurentian Great Lakes using a temporally homogeneous data set. *Journal of Great Lakes Research*, *35*(1), 23–29. https://doi.org/10.1016/j.jglr.2008.11.003

Lawrimore, J., Karl, T. R., Squires, M., Robinson, D. A., & Kunkel, K. E. (2014). Trends and variability in severe snowstorms east of the Rocky Mountains. *Journal of Hydrometeorology*, *15*(5), 1762–1777. https://doi.org/10.1175/jhm-d-13-068.1

Leduc, M., Mailhot, A., Frigon, A., Martel, J.-L., Ludwig, R., Brietzke, G. B., et al. (2019). ClimEx project: A 50-member ensemble of climate change projections at 12-km resolution over Europe and northeastern North America with the Canadian regional climate model (CRCM5). *Journal of Applied Meteorology and Climatology*. https://doi.org/10.1175/JAMC-D-18-0021

Lenssen, N., Schmidt, G. A., Hansen, J., Menne, M., Persin, A., Ruedy, R., & Zyss, D. (2019). Improvements in the GISTEMP uncertainty model. *Journal of Geophysical Research: Atmospheres*, *124*(12), 6307–6326. https://doi.org/10.1029/2018JD029522

Liu, C., Ikeda, K., Rasmussen, R., Barlage, M., Newman, A. J., Prein, A. F., et al. (2017). Continental-scale convection-permitting modeling of the current and future climate of North America. *Climate Dynamics*, *49*(1–2), 71–95. https://doi.org/10.1007/s00382-016-3327-9

Lombardo, K., Colle, B. A., & Zhang, Z. (2015). Evaluation of historical and future cool season precipitation over the Eastern United States and Western Atlantic storm track using CMIP5 models. *Journal of Climate*, *28*(2), 451–467. https://doi.org/10.1175/JCLI-D-14-00343.1

Marciano, C. G., Lackmann, G. M., & Robinson, W. A. (2015). Changes in U.S. East Coast cyclone dynamics with climate change. *Journal of Climate*, *28*(2), 468–484. https://doi.org/10.1175/JCLI-D-14-00418.1

Martynov, A., Laprise, R., Sushama, L., Winger, K., Šeparović, L., & Dugas, B. (2013). Reanalysis-driven climate simulation over CORDEX North America domain using the Canadian Regional Climate Model, version 5: Model performance evaluation. *Climate Dynamics*, *41*(11–12), 2973–3005. https://doi.org/10.1007/s00382-013-1778-9

Martynov, A., Sushama, L., Laprise, R., Winger, K., & Dugas, B. (2012). *Interactive lakes in the Canadian Regional Climate Model, version 5: The role of lakes in the regional climate of North America* (p. 64). Stockholm uni Press. https://doi.org/10.3402/TELLUSA.V64I0.16226

May, R. M., Goebbert, K. H., Thielen, J. E., Leeman, J. R., Camron, M. D., Bruick, Z., et al. (2022). MetPy: A Meteorological Python Library for data analysis and visualization. *Bulletin of the American Meteorological Society*, *103*(10), E2273–E2284. https://doi.org/10.1175/BAMS-D-21-0125.1

McCrary, R., Mearns, L. O., Hughes, M., Biner, S., & Bukovsky, M. S. (2022). Projections of North American snow from NA-CORDEX and their uncertainties, with a focus on model resolution. *Climatic Change*, *170*(3–4), 1–25. https://doi.org/10.1007/S10584-021-03294-8

McCray, C. D., Paquin, D., Thériault, J. M., & Bresson, É. (2022). A multi-algorithm analysis of projected changes to freezing rain over North America in an ensemble of regional climate model simulations. *Journal of Geophysical Research: Atmospheres*, *127*(14), e2022JD036935. https://doi.org/10.1029/2022JD036935

McCray, C. D., Schmidt, G. A., Paquin, D., Leduc, M., Bi, Z., Radiyat, M., et al. (2023). Snowfall statistics for past and future climates calculated from two ensembles of the fifth-generation Canadian Regional Climate Model (CRCM5). [Dataset]. Federated Research Data Repository. https://doi.org/10.20383/102.0743

McCray, C. D., Thériault, J. M., Paquin, D., & Bresson, É. (2022). Quantifying the impact of precipitation-type algorithm selection on the representation of freezing rain in an ensemble of regional climate model simulations. *Journal of Applied Meteorology and Climatology*, *61*(9), 1107–1122. https://doi.org/10.1175/JAMC-D-21-0202.1

McKenna, C. M., & Maycock, A. C. (2021). Sources of uncertainty in multimodel large ensemble projections of the winter North Atlantic Oscillation. *Geophysical Research Letters*, *48*(14), e2021GL093258. https://doi.org/10.1029/2021GL093258

Mearns, L., McGinnis, S., Korytina, D., Arritt, R., Biner, S., Bukovsky, M., et al. (2017). *The NA-CORDEX dataset, version 1.0*. NCAR Climate Data Gateway. https://doi.org/10.5065/D6SJ1JCH

Menne, M. J., Durre, I., Vose, R. S., Gleason, B. E., & Houston, T. G. (2012). An overview of the global historical climatology network-daily database. *Journal of Atmospheric and Oceanic Technology*, *29*(7), 897–910. https://doi.org/10.1175/jtech-d-11-00103.1

Mironov, D., Heise, E., Kourzeneva, E., Ritter, B., Schneider, N., & Terzhevik, A. (2010). Implementation of the lake parameterisation scheme FLake into the numerical weather prediction model COSMO. *Boreal Environment Research*, *15*, 218–230.

Nikulin, G., Lennard, C., Dosio, A., Kjellström, E., Chen, Y., Hänsler, A., et al. (2018). The effects of 1.5 and 2 degrees of global warming on Africa in the CORDEX ensemble. *Environmental Research Letters*, *13*(6), 065003. https://doi.org/10.1088/1748-9326/AAB1B1

Notaro, M., Bennington, V., & Vavrus, S. (2015). Dynamically downscaled projections of Lake-Effect Snow in the Great Lakes Basin. *Journal of Climate*, *28*(4), 1661–1684. https://doi.org/10.1175/JCLI-D-14-00467.1

Notaro, M., Lorenz, D., Hoving, C., & Schummer, M. (2014). Twenty-first-century projections of snowfall and winter severity across Central-Eastern North America. *Journal of Climate*, *27*(17), 6526–6550. https://doi.org/10.1175/JCLI-D-13-00520.1

O'Gorman, P. A. (2014). Contrasting responses of mean and extreme snowfall to climate change. *Nature*, *512*(7515), 416–418. https://doi.org/10.1038/nature13625

Quante, L., Willner, S. N., Middelanis, R., & Levermann, A. (2021). Regions of intensification of extreme snowfall under future warming. *Scientific Reports*, *11*(1), 1–9. https://doi.org/10.1038/s41598-021-95979-4

Reeves, H. D., Elmore, K. L., Ryzhkov, A., Schuur, T., & Krause, J. (2014). Sources of uncertainty in precipitation-type forecasting. *Weather and Forecasting*, *29*(4), 936–953. https://doi.org/10.1175/WAF-D-14-00007.1

Roebber, P. J., Bruening, S. L., Schultz, D. M., & Cortinas, J. V. (2003). Improving snowfall forecasting by diagnosing snow density. *Weather and Forecasting*, *18*(2), 264–287. https://doi.org/10.1175/1520-0434(2003)018⟨0264:isfbds⟩2.0.co;2

Rohde, R. A., & Hausfather, Z. (2020). The Berkeley Earth land/ocean temperature record. *Earth System Science Data*, *12*(4), 3469–3479. https://doi.org/10.5194/ESSD-12-3469-2020

Samenow, J. (2014). *Major winter storm crippling ill-prepared South*. Commutageddon in Atlanta. The Washington Post.

Separovic, L., Alexandrua, A., Laprise, R., Martynov, A., Sushama, L., Winger, K., et al. (2013). Present climate and climate change over North America as simulated by the fifth-generation Canadian Regional Climate Model. *Climate Dynamics*, *41*(11–12), 3167–3201. https://doi.org/10.1007/s00382-013-1737-5

Severson, K. (2014). Atlanta Officials Gamble on storm and lose, and others pay the price.

Thompson, D. W. J., & Wallace, J. M. (1998). The Arctic oscillation signature in the wintertime geopotential height and temperature fields. *Geophysical Research Letters*, *25*(9), 1297–1300. https://doi.org/10.1029/98gl00950

van Vuuren, D. P., Edmonds, J., Kainuma, M., Riahi, K., Thomson, A., Hibbard, K., et al. (2011). The representative concentration pathways: An overview. *Climatic Change*, *109*(1–2), 5–31. https://doi.org/10.1007/s10584-011-0148-z

Verseghy, D. L. (2000). The Canadian land surface scheme (CLASS): Its history and future. *Atmosphere-Ocean*, *38*, 1–13. https://doi.org/10.1080/07055900.2000.9649637

Voldoire, A., Sanchez-Gomez, E., y Mélia, D. S., Decharme, B., Cassou, C., Sénési, S., et al. (2013). The CNRM-CM5.1 global climate model: Description and basic evaluation. *Climate Dynamics*, *40*(9–10), 2091–2121. https://doi.org/10.1007/s00382-011-1259-y

Waskom, M. (2021). Seaborn: Statistical data visualization. *Journal of Open Source Software*, *6*(60), 3021. https://doi.org/10.21105/JOSS.03021

Zarzycki, C. M. (2018). Projecting changes in societally impactful northeastern U.S. Snowstorms. *Geophysical Research Letters*, *45*(12), 67–75. https://doi.org/10.1029/2018gl079820